SANDIA REPORT

SAND98–1654
Unlimited Release
Printed July 1998

Partial Discharge in a High Voltage Experimental Test Assembly

Robert J. Koss, John P. Brainard

Prepared by
Sandia National Laboratories
Albuquerque, New Mexico 87185 and Livermore, California 94550

Sandia is a multiprogram laboratory operated by Sandia Corporation, a Lockheed Martin Company, for the United States Department of Energy under Contract DE-AC04-94AL85000.

Sandia National Laboratories

Issued by Sandia National Laboratories, operated for the United States Department of Energy by Sandia Corporation.

Printed in the United States of America. This report has been reproduced directly from the best available copy.

Available to DOE and DOE contractors from
Office of Scientific and Technical Information
P.O. Box 62
Oak Ridge, TN 37831

Prices available from (615) 576-8401, FTS 626-8401

Available to the public from
National Technical Information Service
U.S. Department of Commerce
5285 Port Royal Rd
Springfield, VA 22161

NTIS price codes
Printed copy: A03
Microfiche copy: A01

SAND 98-1654
Unlimited Release
Printed July 1998

Partial Discharge in a High Voltage Experimental Test Assembly

Robert J. Koss and John P. Brainard
Neutron Tube Development

Sandia National Laboratories
P.O. Box 5800
Albuquerque, New Mexico 87185-0516

Abstract

This study was initiated when a new type of breakdown occurred in a high voltage experimental test assembly. An anomalous current pulse was observed, which indicated partial discharges, some leading to total breakdowns. High voltage insulator defects are shown along with their effect on the electrostatic fields in the breakdown region. OPERA electromagnetic field modeling software is used to calculate the fields and present a cause for the discharge. Several design modifications are investigated and one of the simplest resulted in a 25% decrease in the field at the discharge surface.

Partial Discharge in a High Voltage Experimental Test Assembly

Introduction

This study was initiated when a new type of breakdown occurred in the high voltage experimental test assembly. An anomalous current pulse was observed during operation as the high voltage pulse was applied. A partial discharge occurs when a small region of the distributed capacitance of the test assembly discharges. A capacitive current flows, and charge redistributes on the remaining capacitance, but there is no real charge conduction through the test assembly. A total discharge (breakdown) occurs when a conductive path across the test assembly forms and shorts out the power supply voltage. This breakdown feature is similar to an electron avalanche observed years ago (Brainard and Jensen 1974). However, the insulator in the experimental test assembly was designed such that electric fields force electrons away from the insulator, which prevents electron avalanches.

Analysis of the test assembly shows that an arc occurred between the metal anode housing and the adjacent insulator wall. Figures 1 and 2 are SEM photographs showing the breakdown regions of the insulator and anode respectively. There is probably not enough energy in the partial discharge to do this much damage, i.e., the subsequent total breakdown is most likely the source of energy. The expanding plasma from the partial discharge probably initiates the total breakdown. Relatively large ceramic surface nodules (50 to 100μ) on the insulator in the area near the discharge are shown in figure 3. In the discharge region a significant metal deposit is present, resulting from the breakdown.

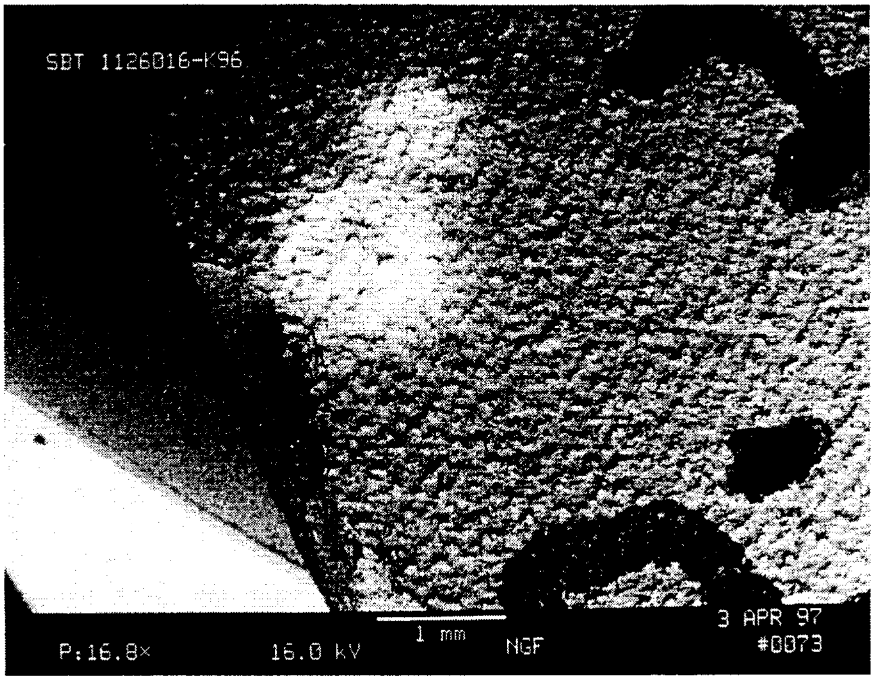

Figure 1. SEM photograph of discharge region of insulator. The light areas indicate breakdown spots. Dark areas are identification marks.

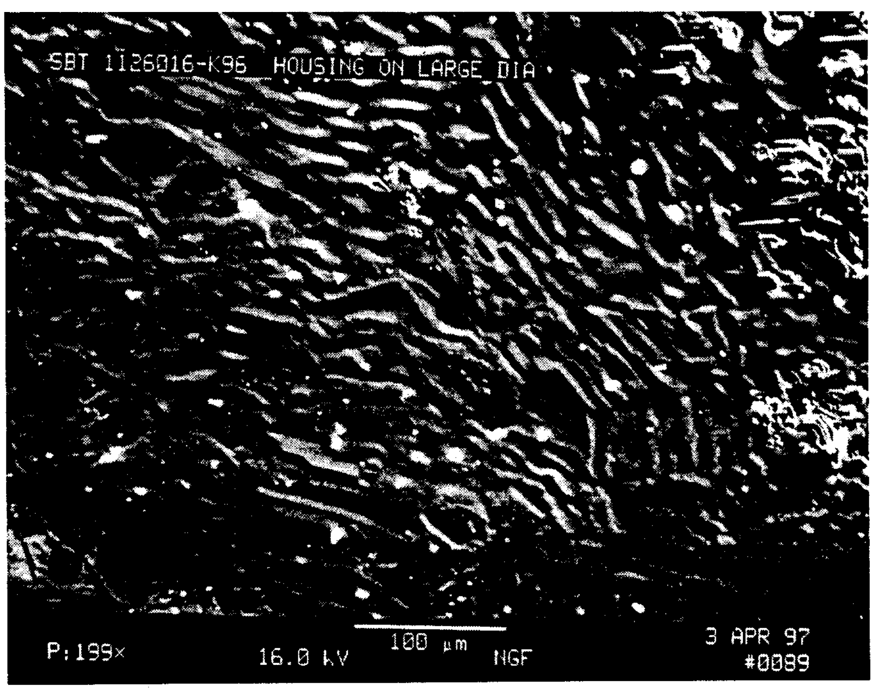

Figure 2. SEM photograph of anode. Wrinkled surface is due to breakdown damage.

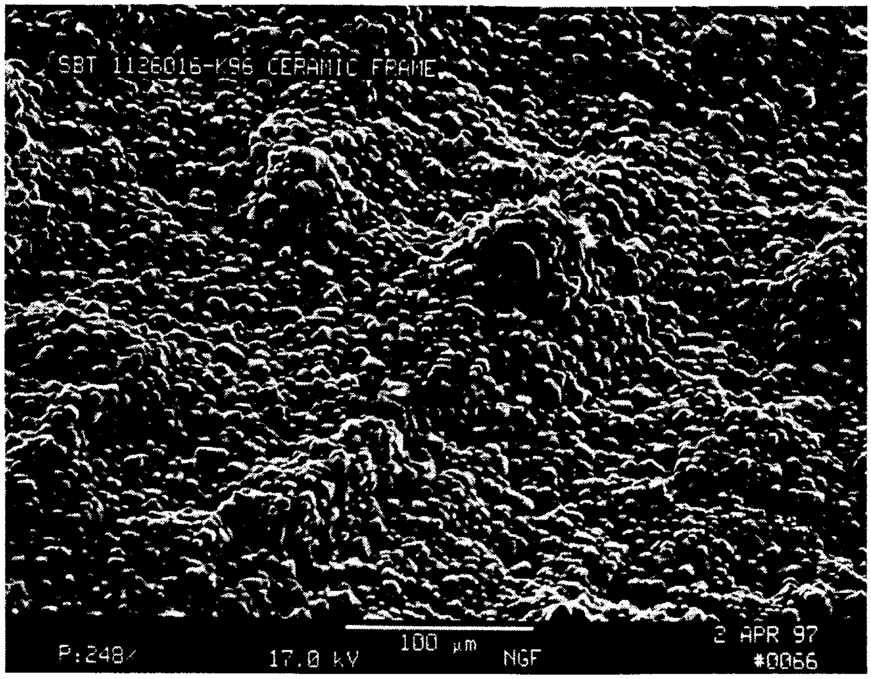

Figure 3. SEM photograph of insulator surface near breakdown damage. Large defects cause field enhancement.

Modeling the Breakdown Region

Figures 4-6 show OPERA electrostatic field models of the partial discharge region of the test assembly. In the partial discharge region, the highest field is on the metal anode, but the area of concern is at the cathode where electron field emission can occur. In general, anode fields play a small role in the pulsed high voltage hold off capability. At the cathode end of the partial discharge the maximum field is 330 kV/cm in vacuum at the insulator surface and 74 kV/cm just inside the bulk insulator. (330 kV/cm at a metallic cathode is considered very high.) Defects such as those shown in figure 3 may produce fields close to the intrinsic dielectric strength of the insulator, which can cause a partial discharge in the insulator and become an electron emitter. While it is well known that metal protrusions from metal electrodes can greatly enhance electric fields (Latham 1981), field enhancements due to metallic or insulator protrusions from an insulator wall have not previously been calculated as far as we know. Figures 7 and 8 show an example of calculations using OPERA and figure 9 summarizes the results. The maximum field enhancement in the vacuum occurs at the tip of the protrusion and in the insulator at the base of the protrusion whether the protrusion is conductive or not. It is clear we could be approaching the intrinsic hold off strength of the insulator. An enhancement of 3.2 with a field of 74 kV/cm gives an actual field of 0.24 MeV/cm, which is the reported dielectric strength for a thin sheet of 94% alumina (Kohl 1967). While a 3-dimensional calculation in the test configuration, at the defect, will be required to determine the exact enhancement, it is clear that enhancement occurs and that a factor of 3.2 is not an unreasonable estimate. We plan to do the OPERA 3-d calculation in the near future.

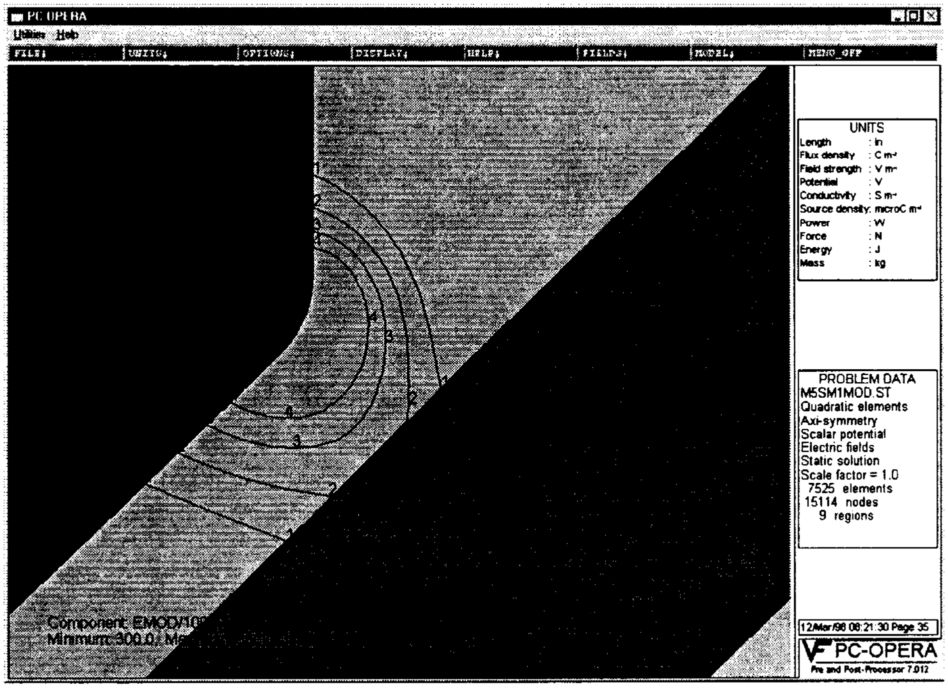

Figure 4. Equal field lines in anode-insulator gap. The anode region is on the left and the insulator is on the right of the field lines.

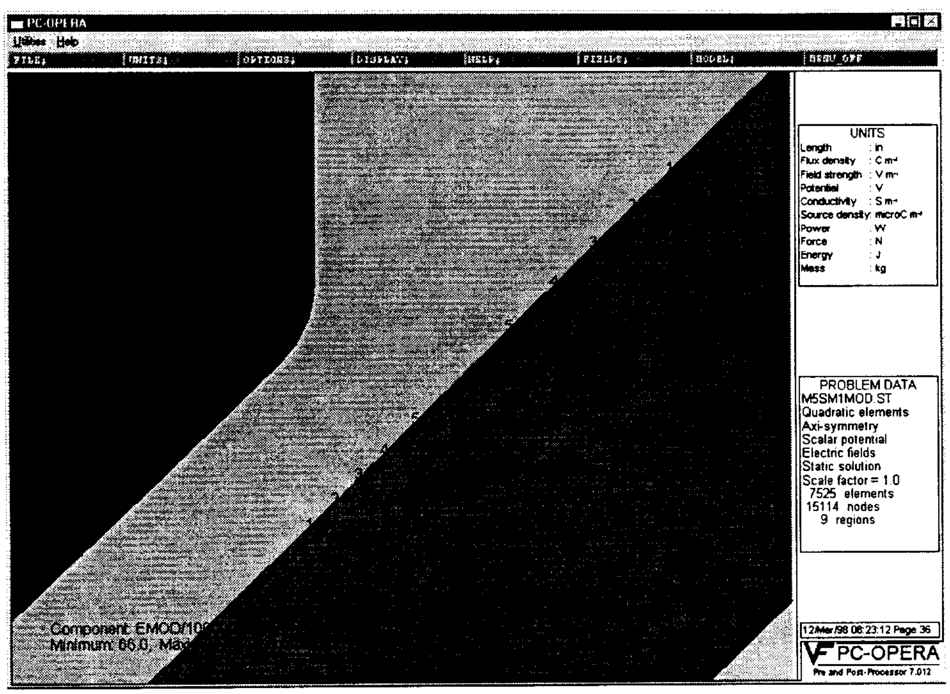

Figure 5. Equal field lines in the bulk insulator.

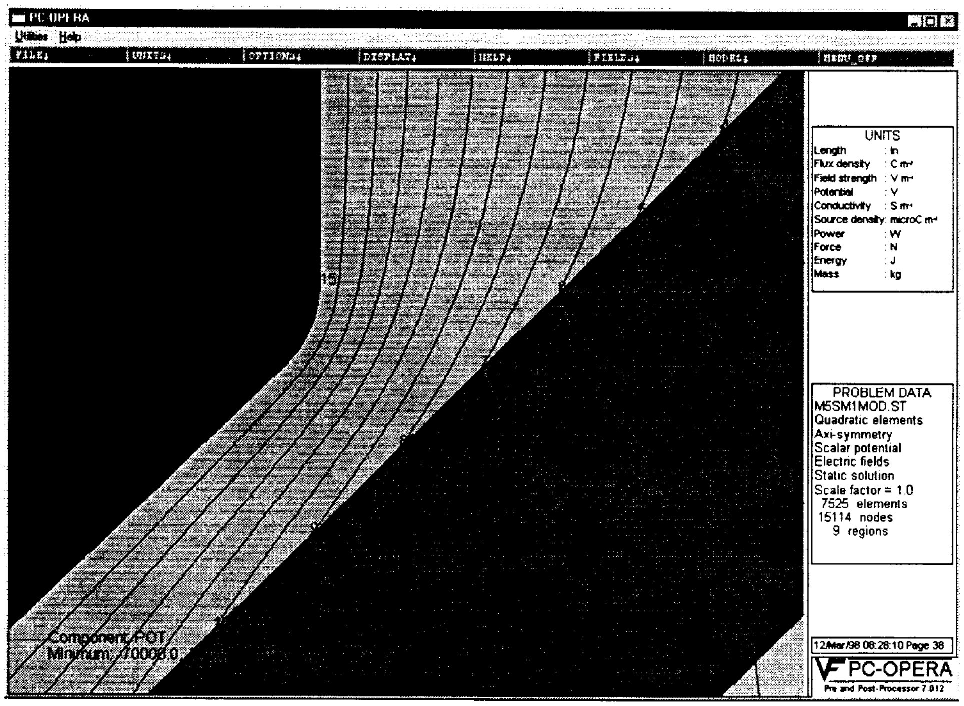

Figure 6. Equi-potential lines at 5 kV/line.

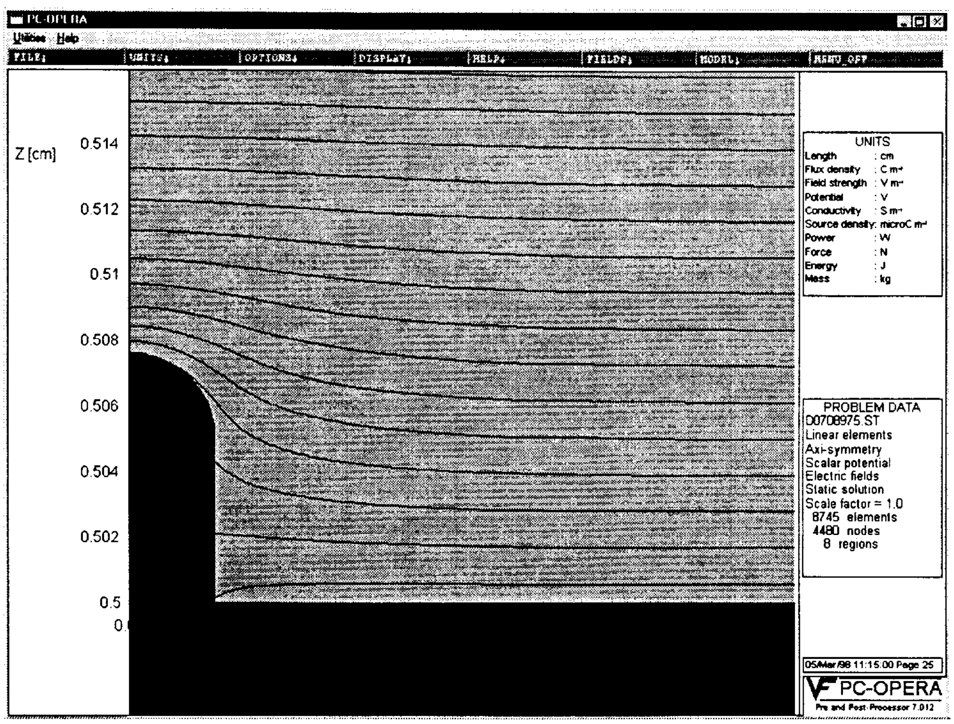

Figure 7. Dielectric protrusion on dielectric surface ε = 10.

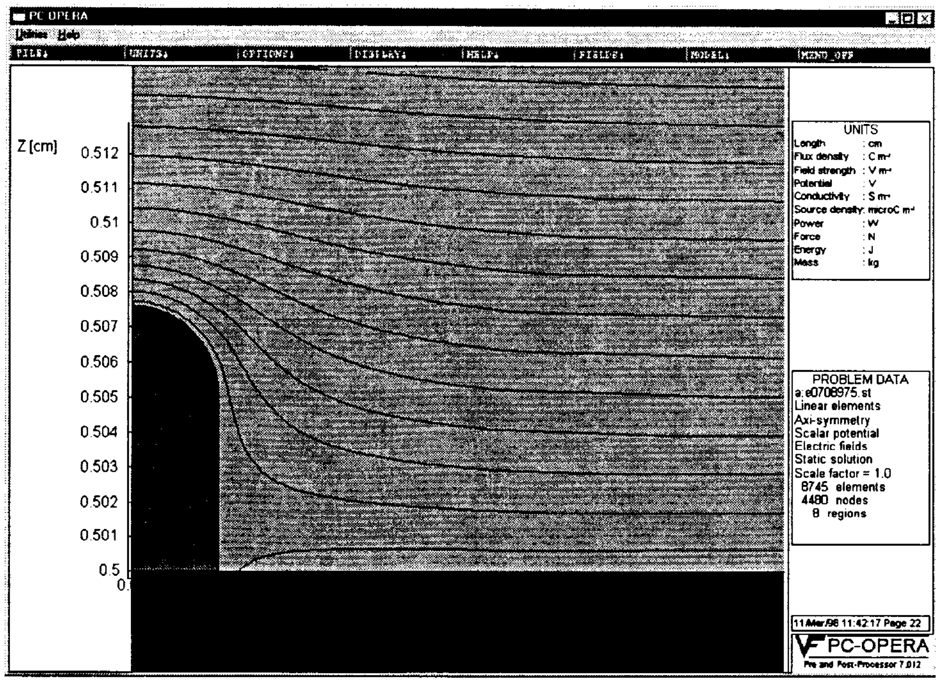

Figure 8. Conductive protrusion on dielectric surface

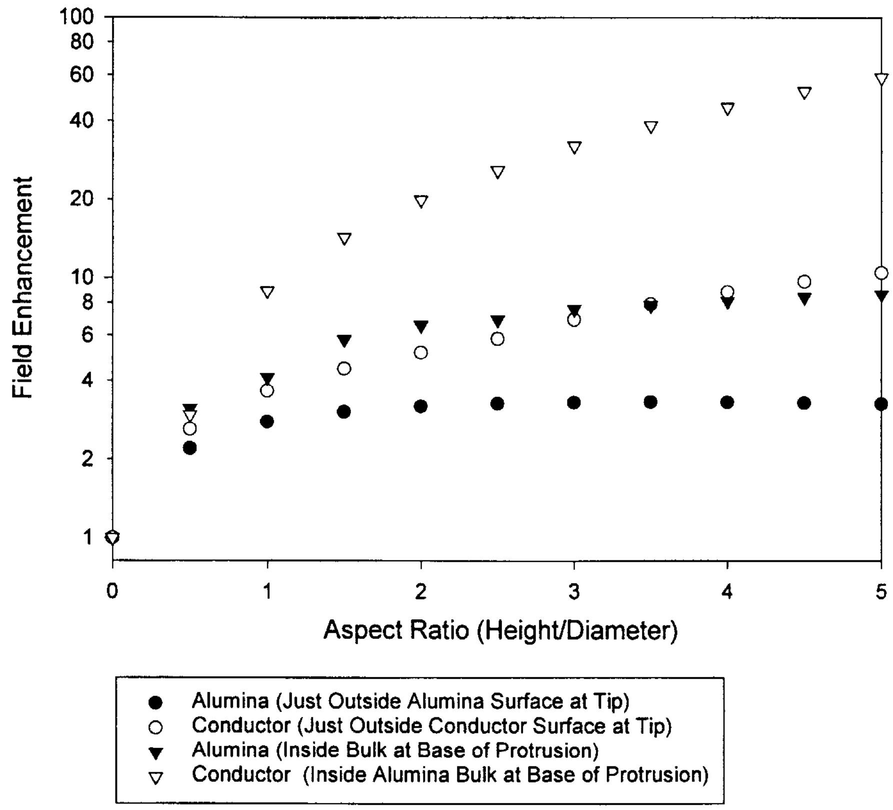

Figure 9. Field enhancements due to conductive and dielectric protrusions on dielectric surface

Discussion of the Breakdown Mechanism

We believe the intrinsic strength of the bulk insulator is reached due to high fields in combination with field enhancement of the protrusions. Electrons are launched from the resulting bulk discharge region either directly or from thermionic emission, and strike the anode at sufficiently high energy to vaporize and ionize the metal. The discharge is then sustained by secondary electrons from the ions striking the insulator. The discharge continues until the fields substantially decrease by the positive charging of the insulator. At this time the fields are nearly parallel to the tapered part of the insulator and electron avalanching can occur. This partial discharge also produces a metal plasma from the anode (we estimate about 50 eV ions) which expands and initiates a complete high voltage breakdown.

Modeling Solutions to the Breakdown

Three ideas to reduce these fields (without major design changes) are examined: (1) smooth the edge of the metal anode by increasing the radius of curvature; (2) increase the spacing between the anode and insulator by decreasing the circumference of the anode and/or increasing the circumference of the insulator; and (3) minimize surface defects, which enhance the electrostatic fields.

Figures 10-15 show field plots of several geometries. A change in anode radius from 30 to 60 mils is modeled in figures 10 and 11. A very small decrease in the maximum field at the insulator results. Figures 12 and 13 combine a 50-mil anode radius (as a worst case for a 60 ± 10 mil specification) and a 5-degree slant, away from the insulator, to increase the anode–insulator distance. Five degrees was chosen since this is the maximum that would allow modification of only a single part. This change lowers the maximum insulator field to 250 kV/cm, an improvement of 25% over the current design. Figures 14 and 15 duplicate figures 12 and 13 plus a 5-degree insulator slant, away from the anode, to further increase the anode–insulator distance. The maximum field here is lowered to 205 kV/cm, for a total improvement of 38%.

Conclusion

It is our judgement that the design change minimizing the impact to the test assembly design is a modification to the anode as in figures 12 and 13. In addition, the insulator vendor is working to improve his technique to minimize defects and meet the drawing surface requirements. With these changes, we believe the partial discharge will be eliminated.

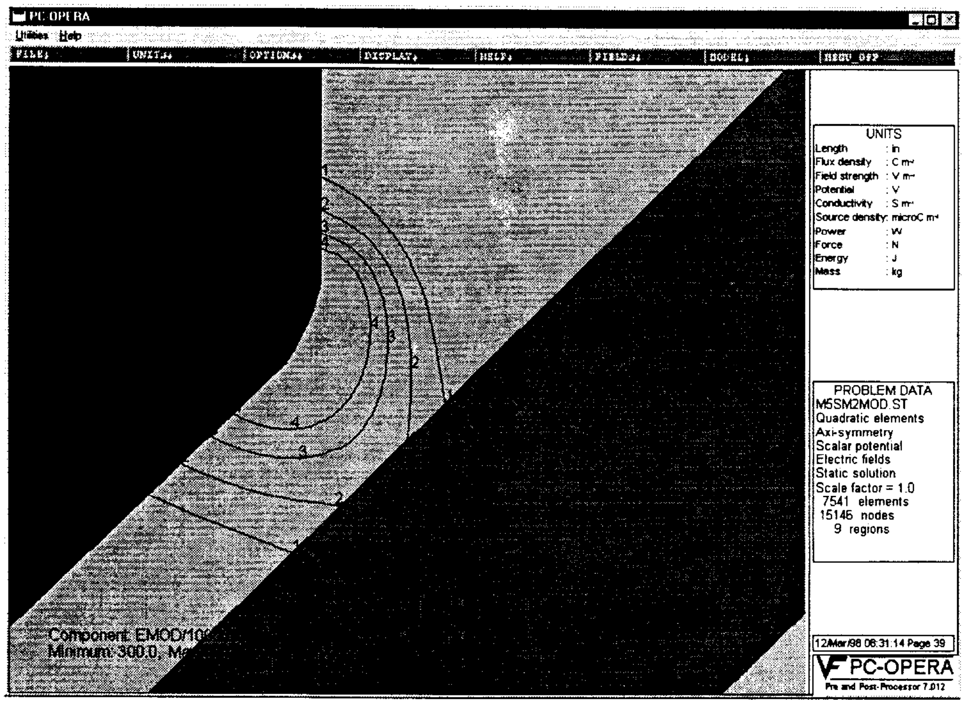

Figure 10. Equal field lines for anode radius of 60 mils.

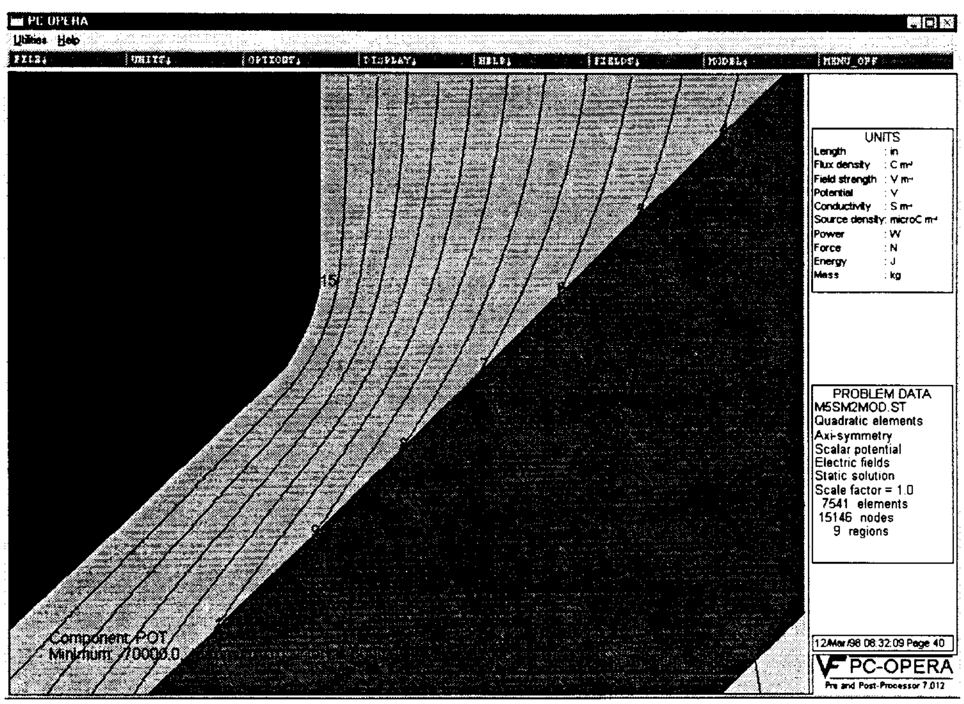

Figure 11. Equi-potential lines for anode radius of 60 mils at 5kV/line.

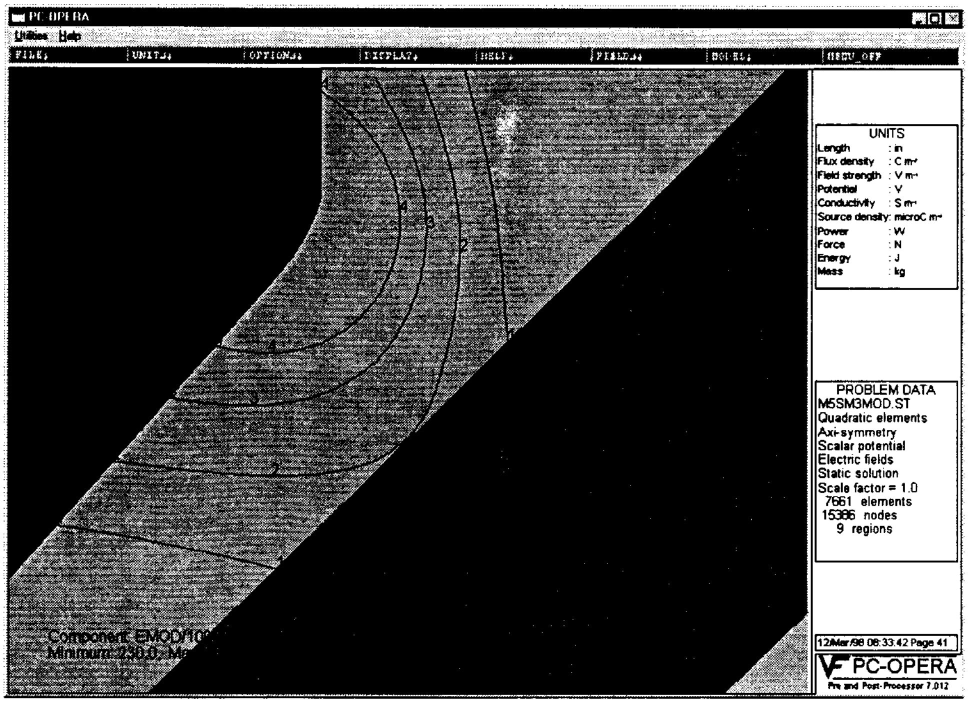

Figure 12. 50 mil anode radius, 5-degree anode slant

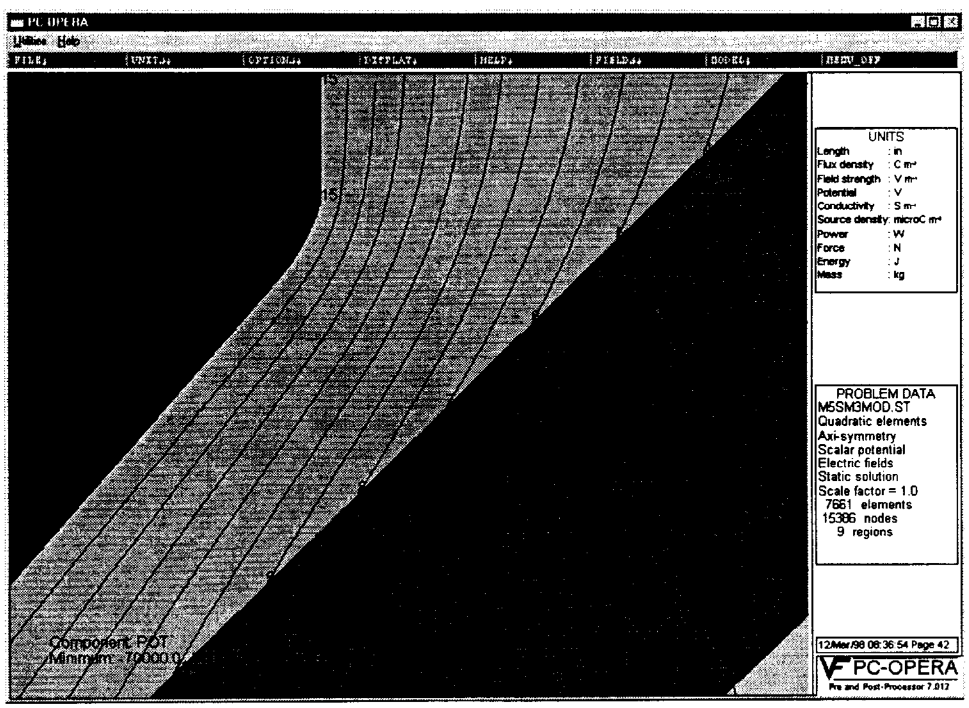

Figure 13. 50 mil anode radius, 5-degree anode slant at 5kV/line

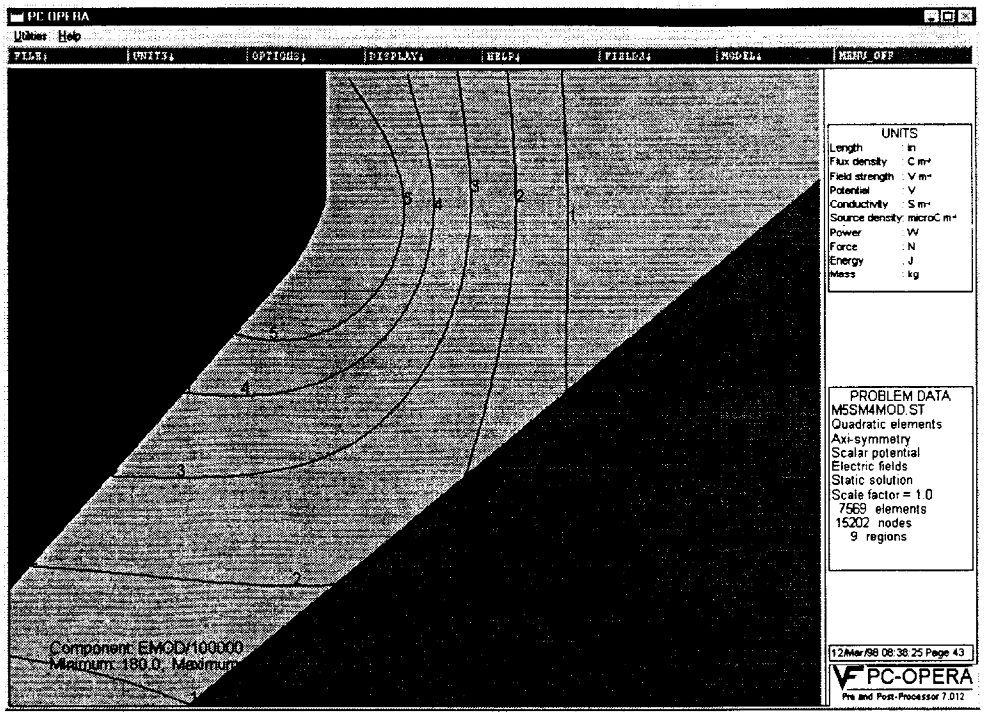

Figure 14. Figure 12 plus 5-degree insulator slant.

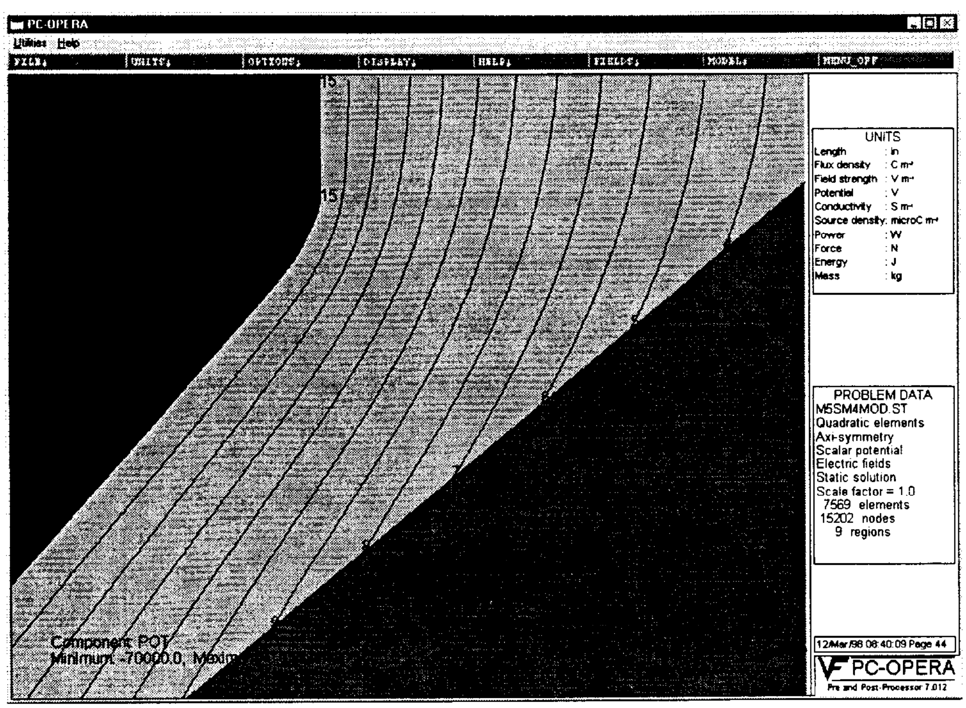

Figure 15. Figure 13 plus 5-degree insulator slant at 5kV/line.

References

J. P. Brainard and D. Jensen, Electron Avalanche and Surface Charging on Alumina Insulators During Pulsed High-Voltage Stress, *J. Appl. Phys.*, 45, 1974.

W. H. Kohl, *Handbook of Materials and Techniques for Vacuum Devices*, Reinhold Publishing Corp., New York, 1967.

R. V. Latham, *High Voltage Vacuum Insulation: The Physical Basis*, Academic Press, Inc., London, 1981.

DISTRIBUTION:

1	MS 0479	PA Sena, 2151
1	MS 0501	PJ Wilson, 1565
1	MS 0513	RJ Eagan, 1000
1	MS 0515	FM Bacon, 1561
1	MS 0515	SG Barnhart, 1561
10	MS 0516	JP Brainard, 1564
1	MS 0516	EJT Burns, 1564
1	MS 0516	CC Busick, 1564
1	MS 0516	CH Draper, 1564
1	MS 0516	GJ Hassig, 1564
10	MS 0516	RJ Koss, 1564
1	MS 0516	GL Laughlin, 1564
1	MS 0516	WP Noel, 1564
1	MS 0516	ML O'Neal, 1564
1	MS 0516	GW Smith, 1564
1	MS 0521	RA Damerow, 1567
1	MS 0521	LD Interrante, 1567
1	MS 0521	TJ Young, 1567
1	MS 0521	DL Wallace, 1567
1	MS 0827	RB Campbell, 9114
1	MS 0827	RO Griffith, 9114

1	MS 0856	L Sena-Rondeau, 14408
1	MS 0869	KG McCaughey, 14400
1	MS 0871	RJ Antepenko, 14405
1	MS 0871	JF Browning, 14405
1	MS 0871	LE Pope, 14405
1	MS 0872	DR Knippel Jr., 14301
1	MS 0873	NE DeMeza, 14302
1	MS 0873	DR McCollister, 14302
1	MS 0873	KW Meredith, 14405
1	MS 0873	MP Senkow, 14302
1	MS 0953	WE Alzheimer, 1500
1	MS 0953	JT Cutchen, 1501
1	MS 1186	ML Kiefer, 9542
1	MS 9036	DR Henson, 2254
1	MS 0918	Central Technical Files, 8940-2
2	MS 0899	Technical Library, 4916
2	MS 0619	Review & Approval Desk, 12690 For DOE/OSTI